

PROGRESS REPORT OF EXPANSION TUBE (TUNNEL) INVESTIGATIONS

By Robert L. Trimpi

NASA Langley Research Center
Langley Station, Hampton, Va., U.S.A.

To be presented at the AGARD Fluid Dynamics Panel Meeting

GPO PRICE \$ _____

CFSTI PRICE(S) \$ _____

Hard copy (HC) 300

Microfiche (MF) 65

ff 653 July 65

Göttingen, W. Germany,
September 14-15, 1967

NATIONAL AERONAUTICS AND
SPACE ADMINISTRATION
WASHINGTON

602-80N

(ACCESSION NUMBER)	(THRU)	(CODE)	(CATEGORY)
29	1	11	
NASA-P-TM-X-60447			
(NASA CR OR TAX OR AD NUMBER)			

PROGRESS REPORT OF EXPANSION TUBE (TUNNEL) INVESTIGATIONS*

By Robert L. Trimpi,
NASA, Langley Research Center, Virginia

September 14, 1967

[REDACTED]


PROGRESS REPORT OF EXPANSION TUBE (TUNNEL) INVESTIGATIONS*

By Robert L. Trimpi
NASA, Langley Research Center, Virginia

INTRODUCTION

The ideal theoretical potential of the expansion tube and tunnel is very great. However, also looming very large are the questions of possible detrimental effects arising from the real physical conditions in which such facilities must operate. The effects of non-ideal diaphragm openings, wall viscosity effects, fluid mixing, contamination, etc., must all be evaluated before the actual operating potential of the expansion tube and tunnel can be established. This report describes the current status of the efforts of the Reentry Physics Branch at Langley Research Center to answer these questions.

No lengthy description of the theoretical performance or cycle description will be presented (see refs. 1-3). However to briefly review the principle of operation, consider the diagrams of figures 1 and 2. The test gas, initially in state ① (fig. 2), is heated and accelerated by a shock wave to state ②. This test gas is further accelerated and simultaneously cooled as it next passes through the unsteady upstream facing expansion wave to the ambient test state ⑤. Testing is accomplished in the time Δt between the passage of the accelerating gas:test gas interface



and the arrival of the trailing edge of the unsteady expansion fan which is being swept downstream by the supersonic flow.

The following sections in this paper will discuss our present knowledge of how the above ideal cycle is modified under actual operating conditions. The data presented herein have been obtained through the efforts of the Hypervelocity Physics Section headed by J. J. Jones who was assisted in overall operation of the expansion tube by J. A. Moore. W. Friesen was project engineer for the velocity profile measurements and K. Haggard was project engineer on the contamination studies.

TEST TIME

Theoretical testing time in the expansion tube is quite small (ref. 1), but may be increased by factors of approximately 3 by either employing simulation techniques (ref. 2) or operating in the expansion tunnel mode (ref. 3). If simulation were combined with expansion tunnel operation even greater increases in test time would be possible but at the expense of other desirable parameters.

Experimental results from the LRC Pilot Expansion Tube (fig. 3), using a low performance driver (room temperature hydrogen at pressures below 1700 psi) indicate test times roughly one to two thirds of the theoretical equilibrium test time for velocities above 20,000 fps (see fig. 4). The test results of figure 4 are for test section ambient temperatures higher than room temperature (i.e., simulation) and since test time is roughly

proportional to the ambient sound speed at a given flow velocity, the test times are correspondingly longer. Solid symbols in the velocity range of 15-17,000 fps indicate test periods limited by the arrival of a pitot pressure dip (which will be discussed in a later section). For this velocity range the test time is much less than the theoretical test time assuming chemical equilibrium.

PITOT PRESSURE CHARACTERISTICS

Magnitude

Another measure of non-ideal effects on expansion tube performance is the pitot pressure magnitude measured at various velocities. Since $p_T \propto \rho_\infty V_\infty^2$, this pressure is also a measure of ambient density. Figure 5 (from ref. 4) indicates a loss of 50 percent from the theoretical equilibrium value for p_T measured on the centerline of the expansion tube. This loss cannot be blamed entirely on non-equilibrium flow since the frozen flow curve also falls above the experimental data. The changes generated by an assumed overtaking downstream expansion wave causing a velocity decrease of 1000 fps, with a corresponding equilibrium decrease in p_T , could apparently account for the behavior of the p_T vs V_∞ curve. However, such an assumed phenomena does not explain the variation in static pressure vs velocity (not shown) and hence its agreement with the p_T vs V_∞ curve must be considered fortuitous.

Fluctuations

Three different levels of pitot fluctuation have been observed in the LRC Pilot Expansion Tube and all are illustrated in figure 6. The high frequency low level fluctuations between the helium:air interface and the arrival of the expansion fan may possibly be an indication of turbulent flow. However, the same gage and mount reproduced the same type of fluctuation in the flow behind the shock wave (not driver gas) of a shock tube at the same unit Reynolds number where laminar flow was expected (ref. 5).

The pitot dip is the next anomaly illustrated in figure 6, and a few general remarks regarding such major departures in pitot pressure behavior are in order before specific LRC results are discussed.

One of the main unexplained phenomena in expansion tube operations has been the occurrence of large temporal irregularities in pitot pressure measurements. Various experimenters have encountered different phenomena. The VKF modified tube produced "spikes" whereas the constant area tube produced none (ref. 6). No abnormal free stream density (and hence pitot) behavior was found at Aberdeen Ballistic Research Laboratories (ref. 7). Experiments at Ames Research Center indicated pitot pressure spikes which occurred after the useful test time had been terminated by arrival of the expansion fan (ref. 8).

The most thorough investigation of the pitot pressure behavior has been executed in the LRC Pilot Expansion Tube and Tunnel. However, boundary

layer effects may be more prominent in this facility since it has a relatively small internal diameter and poor internal surface smoothness. A summary of some main conclusions, based on LRC tests, regarding the pitot dip are listed below:

(1) The dip has not been noted during the theoretical test time for expansion tube operation at ambient test section temperatures required for duplication (i.e., near room temperature). With the current low performance hydrogen driver gas such operating conditions are usually associated with relatively low test section densities and short theoretical test times.

(2) For constant conditions upstream of the secondary diaphragm, the time between shock arrival at the secondary diaphragm and dip arrival at the test section is roughly constant independent of the accelerating gas pressure (p_{10}).

(3) Static pressure records do not always exhibit a concurrent dip; and for those cases which do show a dip, the percentage decrease in static pressure is much smaller than that in the pitot pressure (see fig. 7).

(4) Both pitot and static pressure records show a high frequency hash at arrival of dip in pitot measurements (figs. 6 and 7). This high frequency hash, the third level of pressure fluctuations mentioned earlier, has a much larger amplitude than the initial levels at the beginning of the test gas flow.

(5) The time between arrival of interface (test gas) and dip occurrence is not strongly dependent on the test flow unit Reynolds number over a limited range in Reynolds number.

(6) The shock detachment distance increases (for helium accelerating gas) during dip.

(7) The gas cap radiation decreases during dip.

(8) The dip is not confined to tube centerline but appears near the wall as well.

(9) The dip did not change significantly when the mass (but not rupture strength) of the secondary diaphragm was increased sixfold.

No explanation of this dip which can be substantiated has been found to date. One conjecture associates the dip with boundary layer transition followed by a sudden violent and rapid growth of the boundary layer which results in a bubble of mixed accelerating gas and test gas filling the tube for a short streamwise distance. The pitot dip then would arise from the lowered gas density of the mixture. However, attempts to radiometrically detect the presence of the accelerating gas in the hot gas cap ahead of a pitot probe model have not been successful.

The significance of the pitot behavior to the performance of a full scale hypervelocity expansion tube or tunnel has not yet been established. The data obtained in the pilot facility are at much lower velocity-density combinations than those predicted for the Hot Gas Radiation Research Facility expansion tube, and the required scaling laws have not been determined. Furthermore, the occurrence of a "dip" might not be disastrous if enough useful testing time, which can be as short as a few tens of microseconds, existed either prior to (as in figs. 6 and 7) or following the dip. The dip has occurred in tests to date somewhat after passage of the test gas: accelerating gas interface, so that the attainment of useful test time

appears likely in the expansion tube model. However, since the initial part of the test gas flow is used to establish the nozzle flow in the expansion tunnel mode, later-appearing dips might be a more severe limit in this method of operation.

TEST SECTION VELOCITY PROFILES

Since expansion tube operation requires a long distance of comparatively low Reynolds number flow in the accelerating tube, the effects of viscosity and wall heat transfer might be significant. The LRC velocity measuring technique employs photoionization to initially "tag" a narrow pencil of gas in the test section. A few microseconds later a spark is discharged along the ionized path, and the subsequent reillumination is photographically recorded. Velocity profiles for a range of test section densities for which this technique has been successfully employed are shown in figure 8 for a centerline velocity of approximately 20,000 fps. These profiles show that a relatively flat profile exists across nearly 50 percent of the expansion tube test section, and that as expected the extent of the usable core increases with unit Reynolds number (density). The absolute velocity distribution was found to be constant during the test time.

In the expansion tunnel mode of operation only the inner core of the tube flow is scooped out for expansion in the nozzle (ref. 3). Consequently, based on the above results, the test core in the nozzle will be influenced

primarily by the effective nozzle wall contour (including nozzle boundary layer effects) rather than the viscous effects of the accelerating tube.

A very limited amount of data has been obtained in the expansion tunnel mode by adding to the Pilot Expansion Tube a 10° half-angle conical nozzle with a 2-inch diameter entrance scoop. Records from a pitot pressure rake located 36" from the nozzle inlet, where the geometric nozzle area ratio is about 50, show a nozzle starting process of about 200 microseconds followed by about 200 microseconds of nearly uniform test flow (fig. 9). The origin of the time scale is taken when the initial helium shock wave reaches the pitot rake. The test section velocity was 17,000 fps at a density corresponding to an altitude of 210,000 ft. The three pitot pressure traces have less than 5 percent variation in pressure readings at a given time during the testing period which indicates a fairly flat velocity profile over an eight-inch core.

NON-EQUILIBRIUM FLOW

The maximum dissociation arising during the air processing cycle of the expansion tube or tunnel is much less than that found in shock tunnels for equivalent density-altitude conditions in the test section. This maximum cycle dissociation increases as the nozzle area ratio (\bar{A}) increases for the same equilibrium test section states since a greater part of the expansion occurs in the inefficient steady nozzle expansion rather than the unsteady expansion wave. However, due to the rapid expansion of the working fluid in the expansion tube (tunnel) fan, the possibility of non-equilibrium

test section conditions arises. L. N. Connor has theoretically solved a pertinent modified problem using a non-steady characteristic method including finite rate chemistry. The "air" model employed consisted only of O, O₂, and N₂ and was matched to the same pressure and temperature required by real air behind the primary shock. This approximation results in higher values of X_O for the assumed air compared to real air. Typical results are shown in figure 10 for a test section velocity of 35,000 fps and density equal to air at an altitude of 200,000 ft. The mass fraction of atomic oxygen (X_O) is plotted against the nozzle area ratio (\bar{A}) for the fluid particles which leave the unsteady expansion fan at a distance of 100 ft downstream of the secondary diaphragm. The atomic oxygen decreases as the nozzle area ratio increases because the effect of the longer particle travel time through the expansion fan more than offsets the initially higher X_O at entrance to the expansion fan (note that $X_O \approx .11$ at fan entrance for $\bar{A} = 1$ and increases with \bar{A}). The ratio of energy in O₂ dissociation to the total flow energy is .025, .007, and .0006 for $\bar{A} = 1, 50,$ and 100, respectively. For real air these ratios will be reduced significantly since the computational "model air" neglects NO and thus has too high a value of X_O behind the primary shock; e.g. for $\bar{A} = 1$, "model air" $X_O \approx .11$ contrasted to real air $X_O \approx .05$. The results of this study indicate that non-equilibrium effects in the test section ambient flow should not be large for real air, and that the expansion tunnel will have a lower degree of departure from equilibrium at the end of its test time than an equivalent

length expansion tube. (The tunnel will have a greater departure at the start of the test time when the travel time in the expansion wave is shorter.)

PRELIMINARY CONTAMINATION STUDIES

A principal use of expansion tubes or tunnels will be the study of hot gas radiation wherein even minute quantities of impurities become important if they radiate strongly. Time-resolved spectra have indicated impurity radiation from iron and cyanogen. The preliminary contamination studies reported in this section are concerned only with the identification of possible sources of such flow contaminants. The magnitude, means for elimination, and effects on radiation measurements will not be treated in detail.

The technique employed in the Pilot Expansion Tunnel was as follows: A contaminant patch consisting of a fixed amount of Cesium Nitrate solution was deposited at various locations in the apparatus and the time history of the C_S line radiation at 4593 \AA was monitored during the run by a monochromator-phototube combination with an effective aperture of 1 \AA . Other monochromator channels simultaneously monitored the cyanogen band head at 3883 \AA and the iron line at 3440 \AA . The standard test runs produced a flow velocity of 17,000 fps with nominal test times based on pitot pressure records of approximately 300-400 μsec employing a p_1 of 50 mm. Reference background radiation levels for C_S , obtained by several runs after the tube

had been cleaned and without any C_S patches, are indicated by the cross-hatched area of figure 11.

Briefly summarized below are a portion of the test results using the C_S patch technique and monitoring the radiation from the stagnation region of a blunt model on the tunnel centerline. Note that if one assumes an equilibrium gas, then the maximum radiation shown in figure 11 results from a C_S contamination level of less than 1 particle per million.

(a) C_S on tertiary diaphragm at nozzle entrance: A large amount of radiation was noted as soon as the test gas arrived. The radiation level decayed an order of magnitude in 400 μ secs, but was still approximately 10 to 30 times the clean background level.

(b) C_S on secondary diaphragm: Radiation noted immediately after test gas arrival; the peak radiation level was smaller by an order of magnitude than that for the tertiary diaphragm patch. This radiation decayed by a decade in 250 μ secs to a level approximately three times the clean background, then rose significantly above the background in the expansion fan.

(c) C_S on wall in accelerating chamber ahead of tertiary diaphragm: Radiation level was only slightly above the clean background level.

(d) C_S on wall of intermediate chamber ahead of secondary diaphragm: Radiation increased for 200 μ secs to a value 20 times background, then decayed to nearly background level at 300 μ secs and remained slightly above background level thereafter.

Conclusions which may be drawn from the four studies noted above are:

(a) Contamination from all sources persist throughout an appreciable part of the test flow; (b) Although the maximum relative particle concentration of the contaminant was determined to be very small, the contaminant radiation was relatively strong; (c) Diaphragm contamination is more severe and persistent than wall contamination (for pressure bursting of diaphragms); and (d) Both wall contamination radiation levels drop nearly to the background level at late test times. The importance of electromagnetic diaphragm opening techniques (refs. 3 and 4) or other means of diaphragm removal is evident.

CONCLUDING REMARKS

The expansion tube or tunnel has been shown to be capable of producing hypervelocity flows in density ranges of interest. Test section cores approximately one-half the test section size are typical. The free stream turbulence level does not appear prohibitive. Although test times are short, they are long enough for the establishment of attached flows over many models. Diaphragm contamination still appears to be an unsolved problem for radiation testing if pressure bursting of diaphragms is employed; however, other possibilities for diaphragm removal may alleviate this condition.

REFERENCES

1. Trimpi, Robert L.: A Preliminary Theoretical Study of the Expansion Tube, A New Device for Producing High-Enthalpy Short-Duration Hypersonic Gas Flows. NASA TR R-133, 1962.
2. Trimpi, Robert L.: A Theoretical Investigation of Simulation in Expansion Tubes and Tunnels. NASA TR R-243, 1966.
3. Trimpi, Robert L. and Callis, Linwood B.: A Perfect-Gas Analysis of the Expansion Tunnel, a Modification to the Expansion Tube. NASA TR R-223, 1965.
4. Jones, J. J.: Some Performance Characteristics of the LRC 3-3/4-Inch Pilot Expansion Tube Using an Unheated Hydrogen Driver. Paper presented at the Fourth Hypervelocity Techniques Symposium, Tullahoma, Tennessee, November 15-16, 1965.
5. Jones, Jim J. and Moore, John A.: Exploratory Study of Performance of the Langley Pilot Model Expansion Tube with a Hydrogen Driver. NASA TN D-3421, 1966.
6. Norfleet, Glenn D.; Lacey, John J., Jr.; and Whitfield, Jack D.: Results of an Experimental Investigation of the Performance of an Expansion Tube. Fourth Hypervelocity Techniques Symposium, Tullahoma, Tennessee, November 15-16, 1965.
7. Spurk, J. H. and Bartos, J. M.: Interferometric Measurements of the Nonequilibrium Flow Field Around a Cone. Ballistic Research Lab., BRL R-1333, August 1966.
8. Givens, John J.; Page, William A.; and Reynolds, Robert M.: Evaluation of Flow Properties in a Combustion-Driven Expansion Tube Operating at 7.5 KM/Sec. Fourth Hypervelocity Techniques Symposium, Tullahoma, Tennessee, November 15-16, 1965.

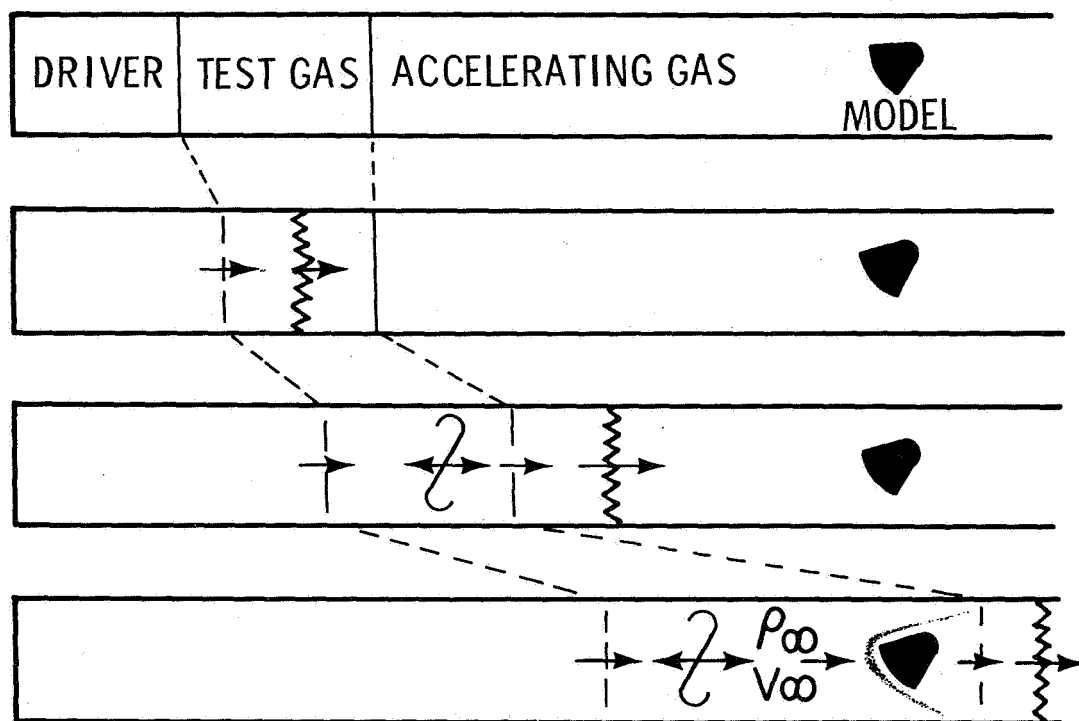


Figure 1.- Expansion tube.

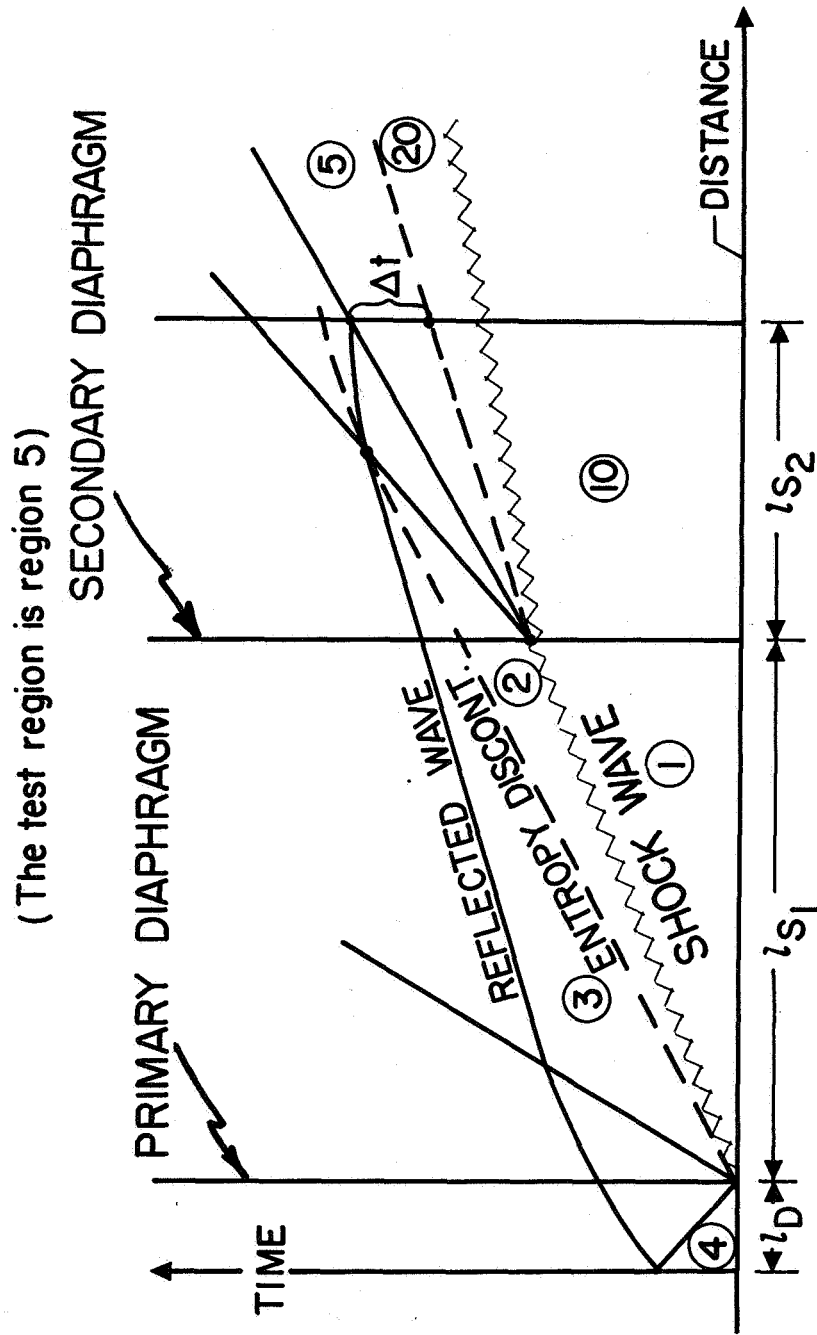


Figure 2.- Distance-time diagram of expansion tube cycle.

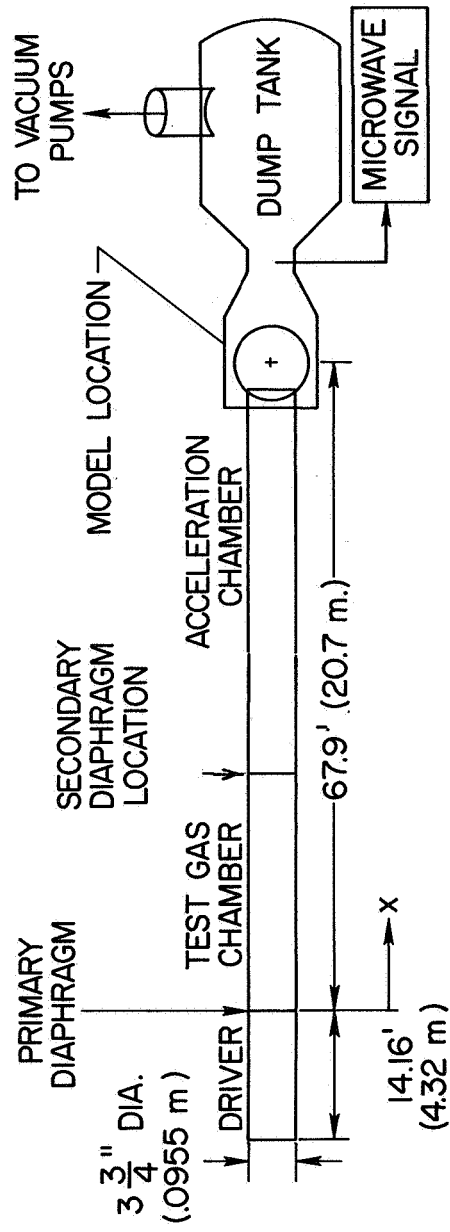


Figure 3.- Langley pilot model expansion tube.

$p_1 = 22 \text{ mm}; l_{s2} = 32 \text{ ft}$

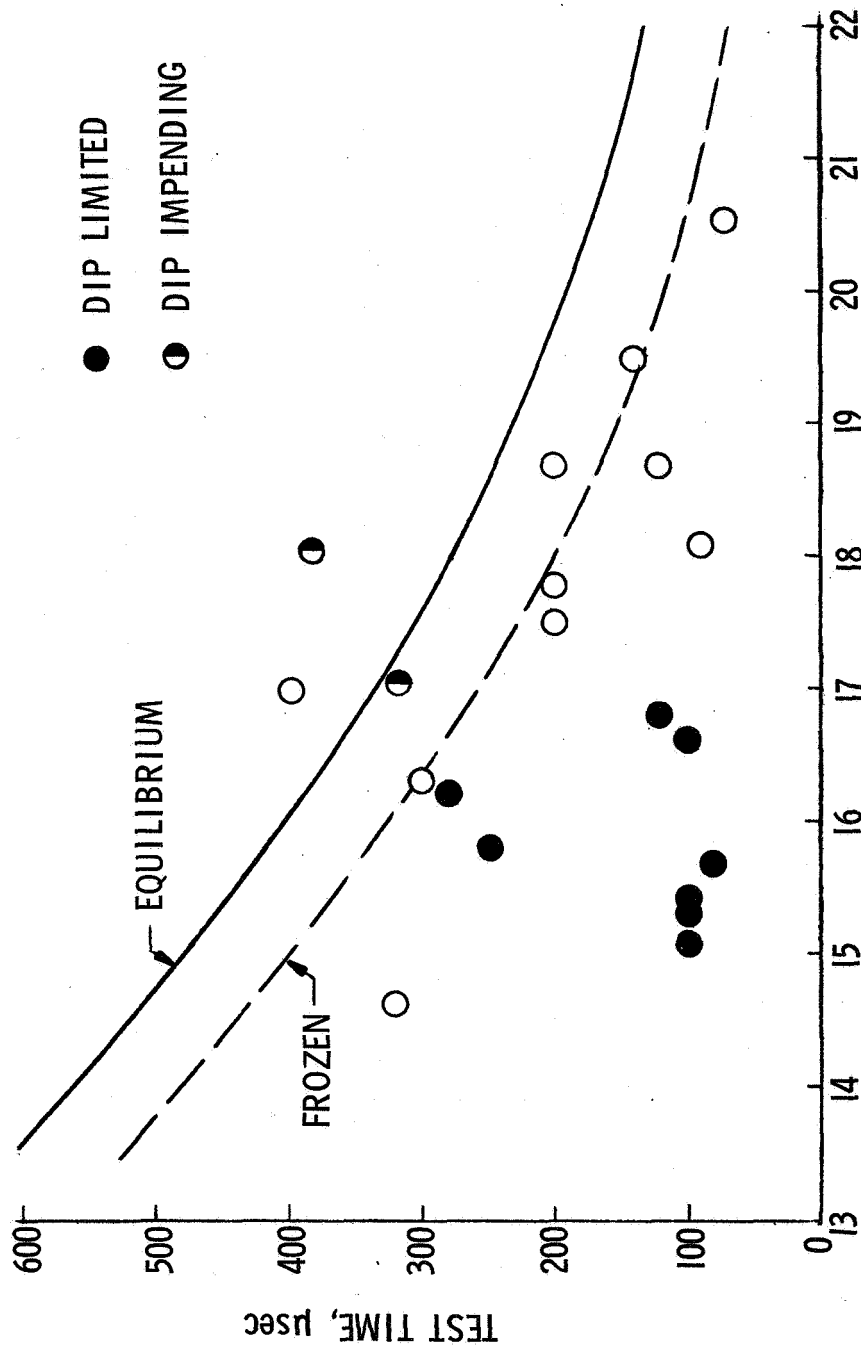


Figure 4.- Test time variation with velocity

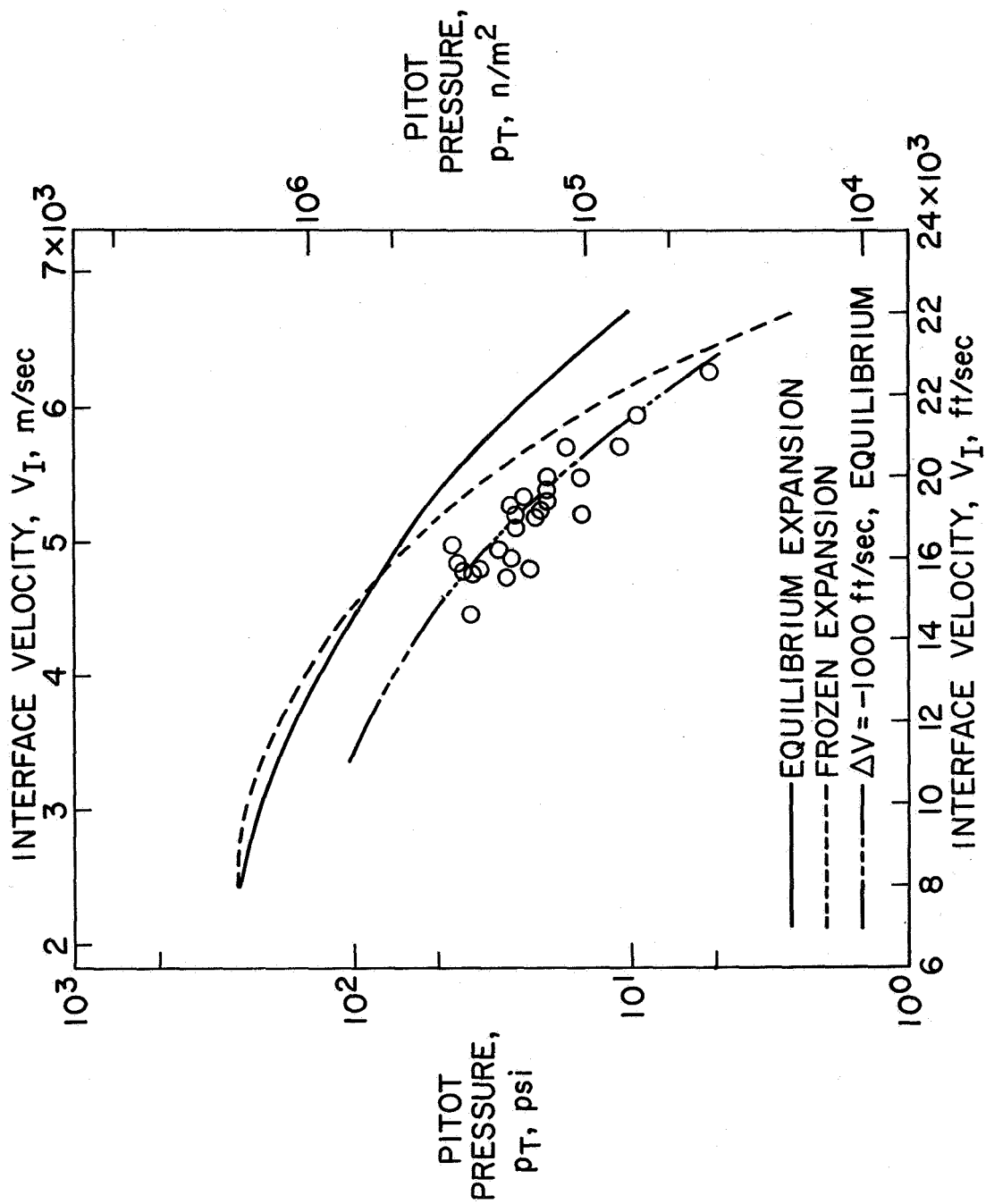


Figure 5.- Test section pitot pressure.

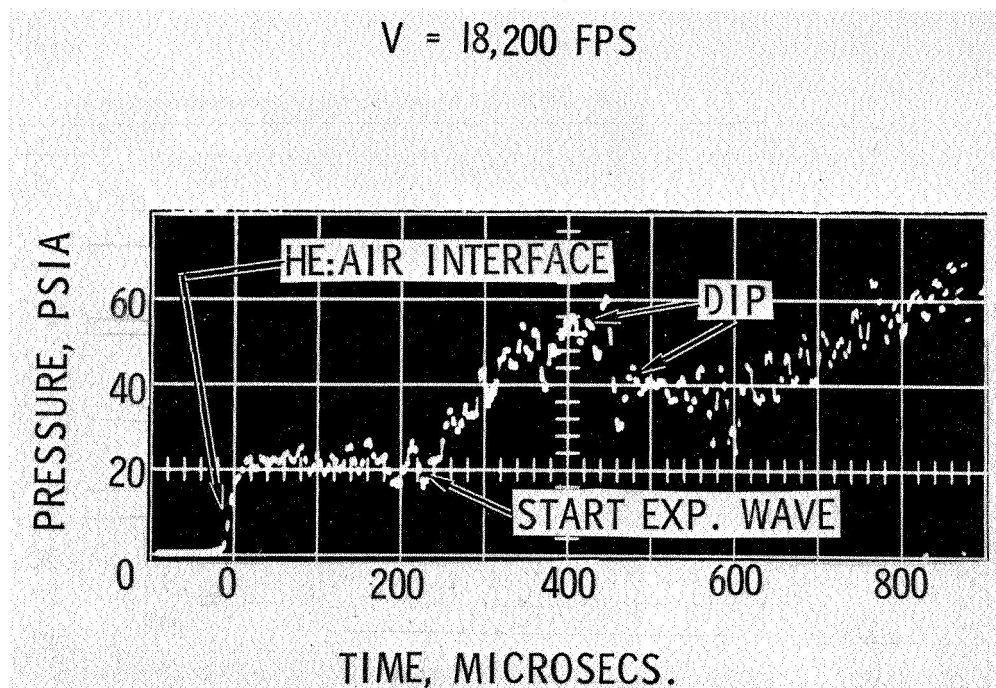


Figure 6.- Expansion tube pitot pressure record.

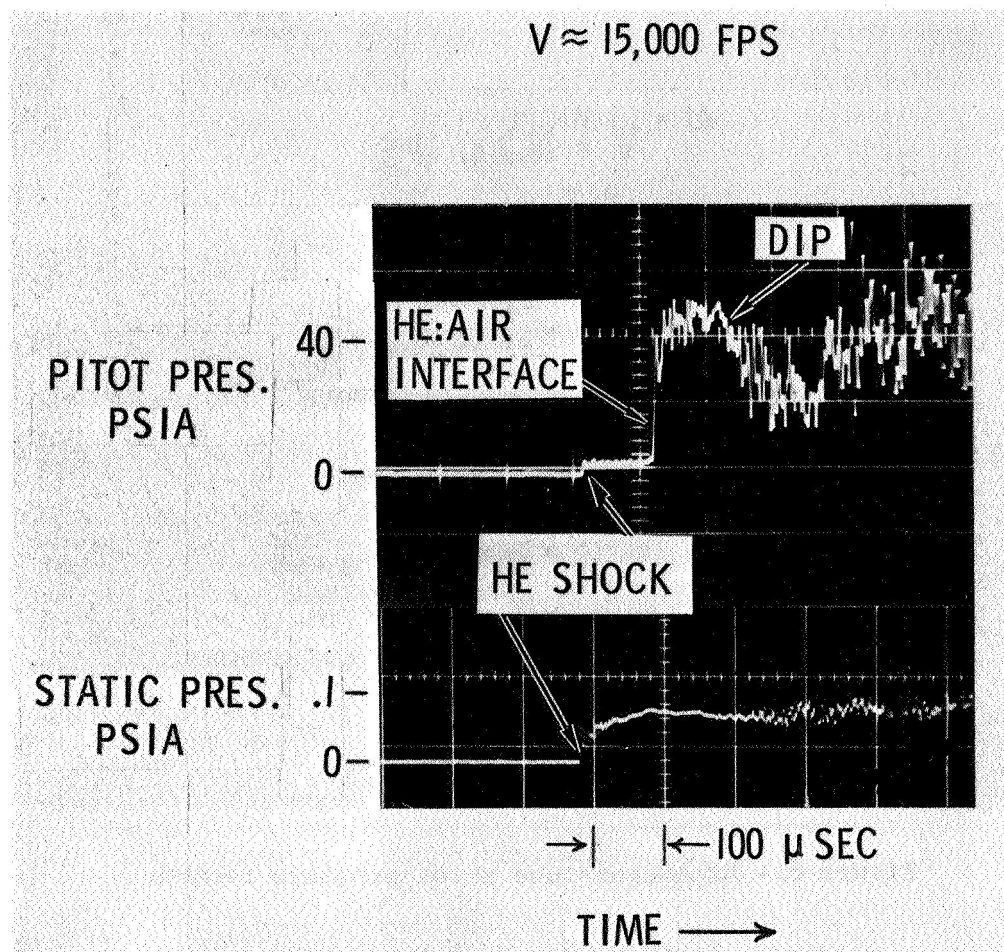


Figure 7.- Expansion tube pitot and static pressure records.

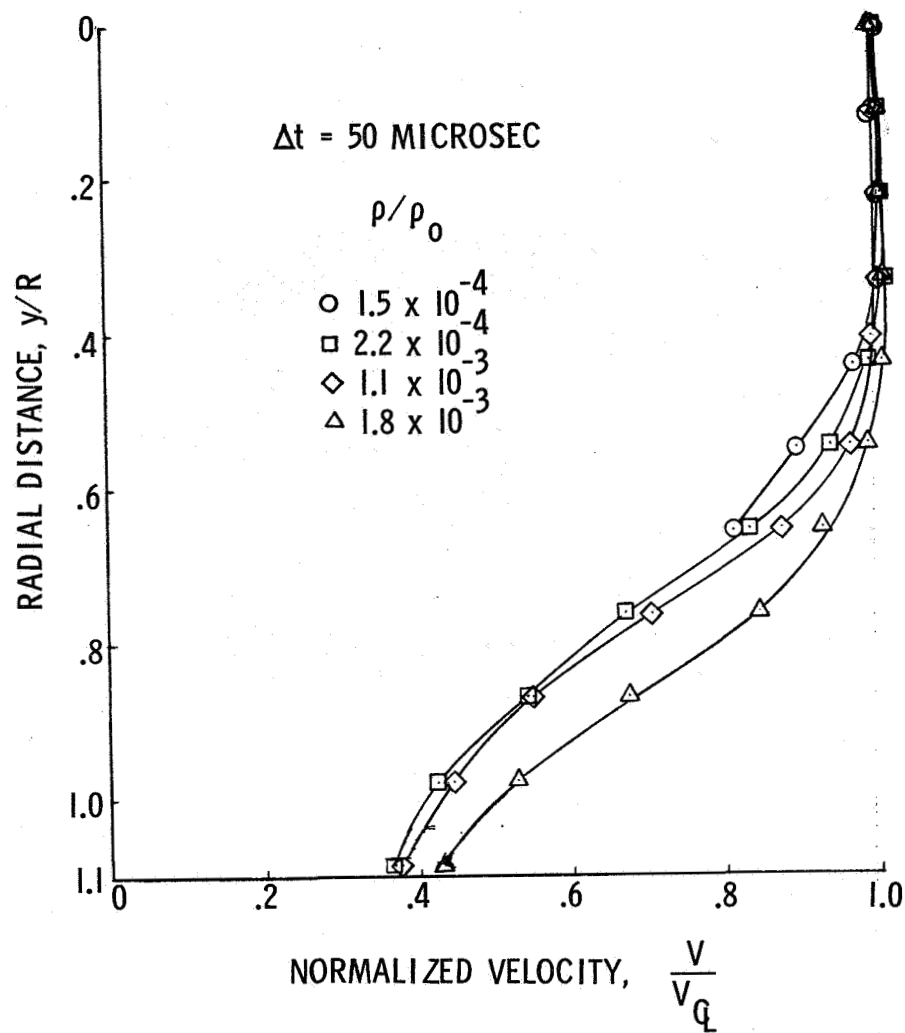


Figure 8.- Velocity profiles in pilot expansion tube open jet test section.

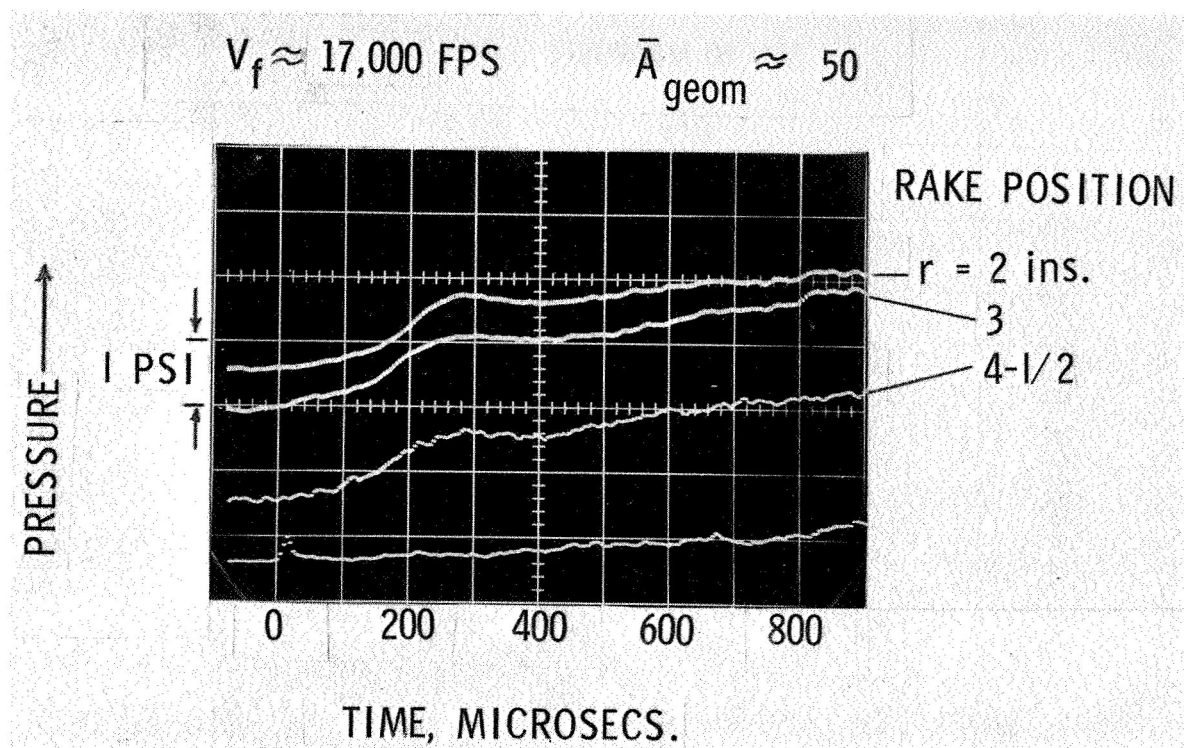


Figure 9.- Expansion tunnel pitot pressure record.

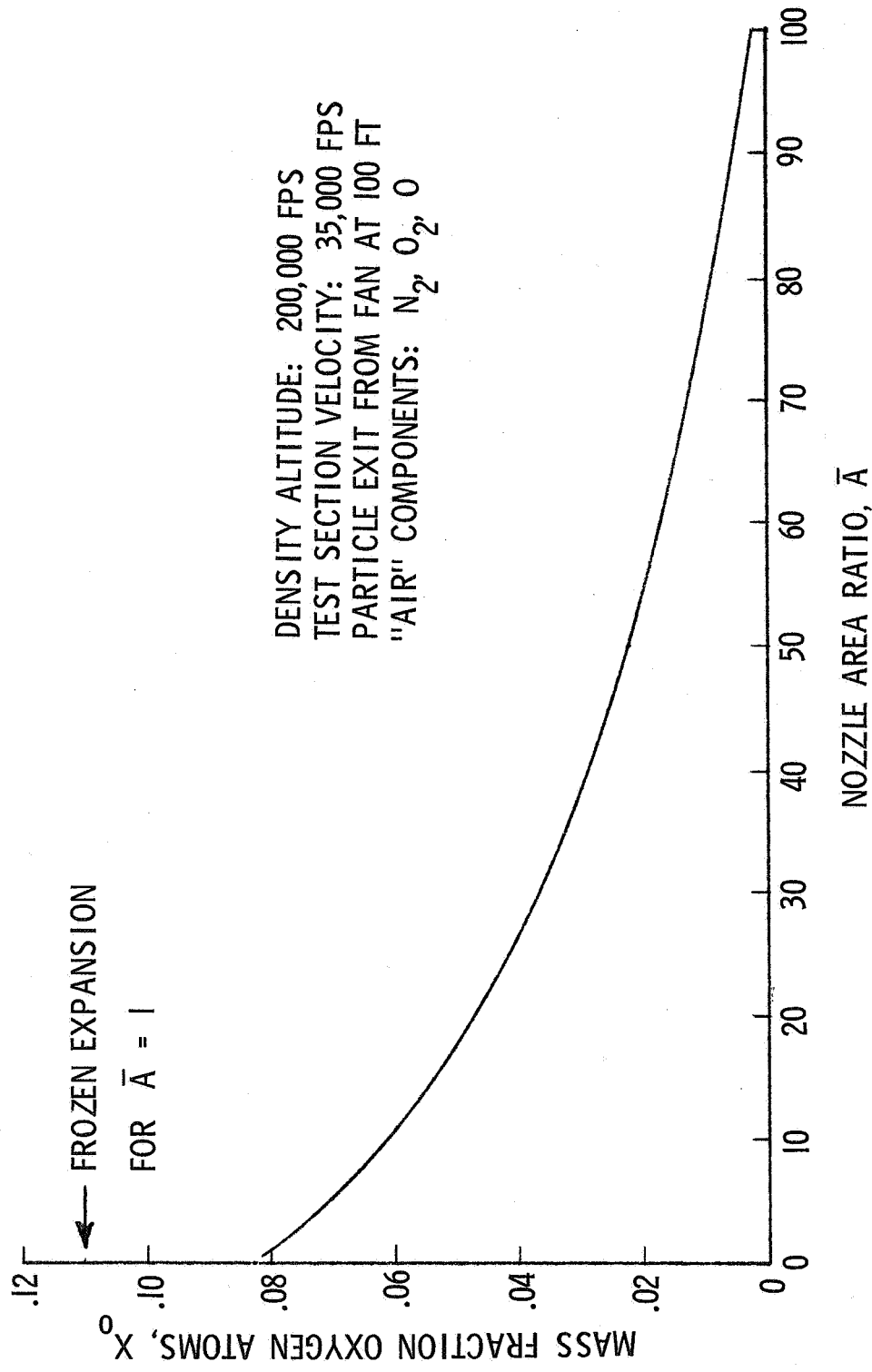


Figure 10.- Effect of finite rate chemistry on test section conditions.

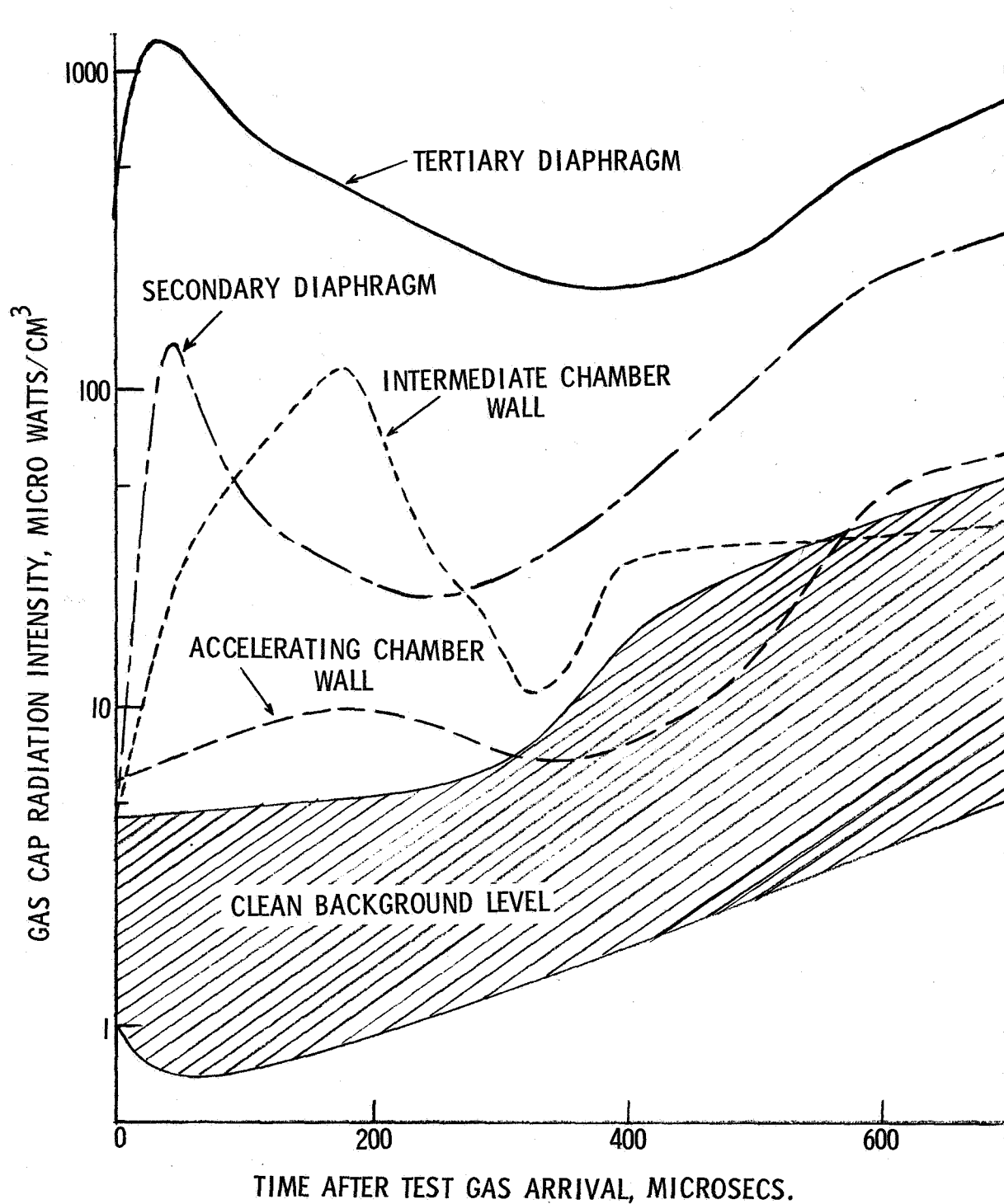


Figure 11.- Cesium nitrate contamination radiation histories.